Analyst

PAPER

View Article Online
View Journal | View Issue

Check for updates

Cite this: *Analyst*, 2026, **151**, 1130

Systematic evaluation of pre-analytical variables on synovial fluid metabolomic profiles using GC-ToF-MS and UHPLC-MS

Yumna Ladha, *[a,b,c] Adam Burke,[c] Nigel Gotts,[c] Royston Goodacre,[c] Karina Wright,[a,b,c] Jade Perry[a,b,c] and Charlotte H Hulme[a,b,c]

Synovial fluid is a clinically valuable biofluid for studying joint diseases through metabolomic analysis. However, given the viscoelastic nature of this biofluid its analysis is challenging. Indeed, the lack of standardised pre-analytical processing protocols for synovial fluid metabolomics potentially introduces significant variability that can compromise data reliability and hinder the application/interpretation of results. This study systematically assesses how common sample handling variables including sample dilution, freeze–thaw cycling, blood staining and viscosity reduction (*via* hyaluronidase digestion and bead beating) affect the metabolomic profile of synovial fluid. Using a combination of untargeted GC-ToF-MS and UHPLC-MS (in both electrospray ionisation modes; ESI+ and ESI–) for the profiling of both polar and non-polar metabolites, we evaluated changes in detectable metabolite numbers, small molecule class distribution and relative abundances in a collection of synovial fluid samples. Sample dilution had the most pronounced impact on metabolite read-outs, significantly reducing detectable metabolite numbers. Blood staining introduced distinct metabolites and resulted in the artificial increase in the relative abundance of three metabolites including adenine, hypoxanthine and 4-fluoro-DL-tryptophan. Bead beating enhanced the detection of a broad range of lipid species particularly in the UHPLC ESI+ analysis. Freeze–thaw cycling and hyaluronidase treatment had minimal effects on overall metabolite quantities or composition. These findings underscore the importance of optimising and standardising synovial fluid sample handling to ensure reproducibility and to enable accurate interpretation of metabolomic data for the study of disease mechanisms and biomarker discovery.

Received 3rd September 2025,
Accepted 8th December 2025

DOI: 10.1039/d5an00943j

rsc.li/analyst

Open Access Article. Published on 21 January 2026. Downloaded on 2/26/2026 9:07:48 AM.
This article is licensed under a Creative Commons Attribution-NonCommercial 3.0 Unported Licence.

Introduction

Synovial fluid (SF) is a viscoelastic biological fluid found in the cavities of synovial joints such as the hip and knee. SF plays a crucial role in joint lubrication, nutrient supply to articular cartilage (AC), and waste removal.[1,2] The interaction between SF and the surrounding tissues like the synovium and AC makes the fluid reflective of joint health and pathological processes.[3] Additionally, the synovial membrane allows for the diffusion of molecules such as cytokines and growth factors from the plasma into the SF therefore further contributing to its dynamic composition.[4] Analysing its composition can provide valuable insights into the pathophysiology of various joint diseases, including osteoarthritis, rheumatoid arthritis, and septic arthritis and can aid in the identification of potential biochemical biomarkers.[5,6] Biochemical biomarkers include a wide range of both large and small molecules and can be used for diagnostic, prognostic, predictive and therapeutic purposes.[7] Metabolomics can be used to profile SF to inform on altered joint metabolism and to identify biomarkers which are reflective of the endogenous and exogenous contributors to joint diseases.[8] Analytical techniques that have commonly been used to characterise the metabolome of complex biofluids such as SF include gas chromatography-mass spectrometry (GC-MS), and liquid chromatography-mass spectrometry (LC-MS) based metabolomics.[9,10]

Collection of human SF can be technically challenging, particularly in the absence of effusion (the abnormal accumulation of fluid). SF is typically collected at the time of surgery or through joint aspiration.[11] If effusion is not present and SF volumes are small, various techniques that include lavage/wash-out of the joint have been implemented to acquire a dilute SF sample.[12–14]

During SF collection and subsequent processing, numerous pre-analytical factors can alter the metabolomic composition,

[a]*Oswestry Keele Orthopaedic Research Group (OsKOR), Robert Jones and Agnes Hunt Orthopaedic Hospital Foundation Trust, Oswestry, Shropshire, UK. E-mail: c.hulme1@keele.ac.uk*
[b]*Centre for Musculoskeletal Health, Keele University, Staffordshire, UK*
[c]*Centre for Metabolomics Research, Department of Biochemistry, Cell and Systems Biology, Institute of Systems, Molecular and Integrative Biology, University of Liverpool, Liverpool, UK*

This journal is © The Royal Society of Chemistry 2026

Open Access Article. Published on 21 January 2026. Downloaded on 2/26/2026 9:07:48 AM. This article is licensed under a Creative Commons Attribution-NonCommercial 3.0 Unported Licence.

complicating reliable comparison and quantification across samples. There are currently no published standard protocols for the preparation of SF for metabolomic analysis using GC-MS nor LC-MS. SF typically presents as a pale-yellow colour however in some cases it presents with blood staining that could be caused by a range of factors both traumatic (sample aspiration process, surgery, fractures *etc.*) or non-traumatic (bleeding disorders) and inflammatory processes such as synovitis, which increase synovial membrane permeability allowing cells from the blood to enter the synovial cavity.[13,15,16] The presence of blood in SF introduces the risk of altering the metabolite profile due to haemolysis. Haemolysis can result in the release of intracellular metabolites and enzymes such as tryptophan phospholipids from the cellular membrane therefore contaminating the SF.[17] In this study, the term blood stained refers to SF samples contaminated with blood that remained visibly red after centrifugation, indicating haemolysis and the release of intracellular contents. This terminology reflects our clinical observations, where haemolytic SF aspirates are occasionally encountered during joint aspiration procedures.

As lavage is often required in the absence of effusion, the collected SF is diluted theoretically resulting in the reduced concentration/loss of metabolites, thus risking analyte signals in the samples approaching or falling below limits of detection when analysed using GC/LC-MS/MS. This makes it difficult to distinguish metabolite signals from background noise making the data unreliable and unreproducible.[18] Where SF is not diluted with saline, the volume of sample is limited (median total knee volume = 3.05 mL),[19] therefore, the limited availability of the precious clinical samples often necessitates their use in multiple analyses, making freeze–thawing unavoidable. SF is highly viscous, mainly due to high hyaluronan content (1–4 mg mL^{-1} (ref. 20)), other glycoproteins such as lubricin also contribute to its viscoelastic properties.[21] Enzymatic digestion with hyaluronidase is therefore commonly applied to homogenise and reduce the viscosity making the biofluid easier to work with.[22] Hyaluronidase treatment has the additional benefit as shown in proteomic studies of improving the detection of immune cells.[23,24] However, the benefits/drawbacks of this technique, or other physical methods such as bead beating to reduce viscosity, when applied for the metabolomic profiling of SF using a mass spectrometry approach has not been explored.

The influence on metabolite stability due to pre-analytical sample conditions and handling has been widely explored in various biospecimens including serum, plasma and urine.[25–28] Although pre-analytical handling has been estimated to account for up to 80% of experimental irreproducibility[29] only a few studies have directly examined how handling and storage conditions influence the stability of metabolites in SF; notably all of which have been measured using NMR. Early NMR-based investigations demonstrated that SF metabolites remain stable under controlled freezing and short-term storage,[30] while more recent work has shown that controlled enzymatic and physical processing has limited impact on small-molecule composition.[31] Jaggard *et al.*[32] further provided a comprehensive review and experimental evaluation of pre-analytical factors including storage temperature, freeze–thaw cycling, and collection procedures highlighting that although studies have addressed either directly or indirectly these variables, few have quantified their effects systematically.

The present study builds on this evidence by systematically assessing multiple common pre-analytical variables using complementary GC-MS and LC-MS platforms, an approach not previously undertaken. This is important as NMR and MS techniques provide complementary insights into the metabolome: NMR spectroscopy enables quantification of abundant small molecules whereas MS based techniques offer greater sensitivity and coverage of chemically diverse, low abundance metabolites.[33,34] Previous investigations on biofluids such as plasma and serum have demonstrated that NMR and MS based metabolomics highlight different aspects of the metabolome in response to pre-analytical handling factors therefore highlighting the need to assess these effects on the SF metabolome using MS based techniques to complement existing knowledge derived primarily from NMR studies.[35–38]

The condition of the sample as well as its handling, including collection, processing, storage, and preparation, are well-recognised sources responsible for the highest variations observed in metabolomic studies.[39] This can significantly impact the accuracy and reliability of downstream GC-MS and LC-MS analyses, potentially leading to misinterpretation of results and inaccurate clinical/scientific conclusions. Therefore, understanding the effects that sample condition has on metabolite stability and optimising sample handling procedures is critical to ensure the integrity and quality of SF samples and to maximise the information obtained from these sophisticated analytical techniques.[40]

This study aimed to determine how common pre-analytical variables: blood contamination, dilution, freeze–thaw cycles, and viscosity treatments (hyaluronidase digestion and bead beating) influenced the detectable metabolomic profile of SF. We sought to assess changes in both metabolite abundance and class representation using GC-MS and LC-MS/MS platforms.

Methods

Synovial fluid and blood collection and storage

Ethical approvals were obtained from the National Research Ethics Service – North West Committee (11/NW/0875). SF and blood samples were collected from patients who had provided informed consent. SFs were collected between the years 2017–2024. SFs were aspirated from knee joints at the time of total knee replacement (TKR) surgery except for one which was obtained *via* a synovial biopsy at the Robert Jones and Agnes Hunt Orthopaedic Hospital. Samples were aspirated using sterile polypropylene syringes and transferred to sterile polypropylene 30 mL tubes. Samples were kept at room temperature until processing which occurred within 30 min of collection. The centrifuge used for SF samples was not temperature controlled. Following centrifugation at 6000*g* for 15 min, the SF was aliquoted in CryoPure tubes (2 mL tube, SARSTEDT AG

Open Access Article. Published on 21 January 2026. Downloaded on 2/26/2026 9:07:48 AM.
This article is licensed under a Creative Commons Attribution-NonCommercial 3.0 Unported Licence.

& Co. KG) and stored at −80 °C for up to 6 months, followed by long term storage in liquid nitrogen. Patient matched blood samples were collected in EDTA coated tubes and centrifuged at 6000*g* for 15 min at 4 °C before collecting the plasma free whole blood aliquoting for storage at −80 °C.

Sample preparation

The variables that were tested included the effect of freeze–thaw cycles, dilution, viscosity reduction and blood contamination (Fig. 1). Five patient samples were assessed across each test group for this experiment. The control group consisted of a neat SF sample that underwent one freeze–thaw cycle, with no blood contamination or viscosity reducing treatment.

Freeze–thaw cycling

SF aliquots of 100 μL were exposed to either two or three freeze–thaw cycles. Samples were thawed on ice for 30 min until fully thawed before being returned for storage at −80 °C. Each freeze–thaw cycle was carried out on a separate day.

Sample dilution

Dilution effect was determined *via* the mixing of the sample with 0.9% physiological saline solution (DEMO S.A., Greece (as used clinically)) at a 1 : 5, 1 : 10 or 1 : 20 ratio. Samples were diluted on ice prior to analysis.

Blood staining

SF samples were thawed on ice following which approximately 20 μL of patient-matched whole non-haemolysed blood was added to the samples. Samples were incubated on ice for 20 min before being centrifuged at 3000*g* for 15 min. The supernatant was collected and stored at −80 °C.

Hyaluronidase treatment

SF aliquots of 100 μL were exposed to enzymatic pre-treatment using hyaluronidase (Sigma-Aldrich, Product number: H6254). Samples were incubated at room temperature with 3.3 μL of hyaluronidase (200 units per mL) for 1 h before being centrifuged at 1000*g* for 5 min following which the supernatant was collected. Samples were then kept on ice until further analysis within 1 h.

Bead beating

The supernatant of samples undergoing bead beating was collected post sample quenching/extraction and transferred to bead beating vials (2 mL Tube 1.4 Ceramic, Cat No. 15555799, Fisher Scientific). Samples underwent two rounds of 8 s beating cycles with a 10 s pause in between each cycle at 19 °C (Bead Mill 24 Homogenizer, Fisher Scientific, Loughborough, UK) before transferring the samples into 2 mL Eppendorf tubes for centrifugation.

Reagents

All internal standards were obtained from Cambridge Isotopes (Tewsbury, MA). All other chemicals were obtained from Fisher Scientific (Loughborough, UK) and are of Optima LC-MS grade where available.

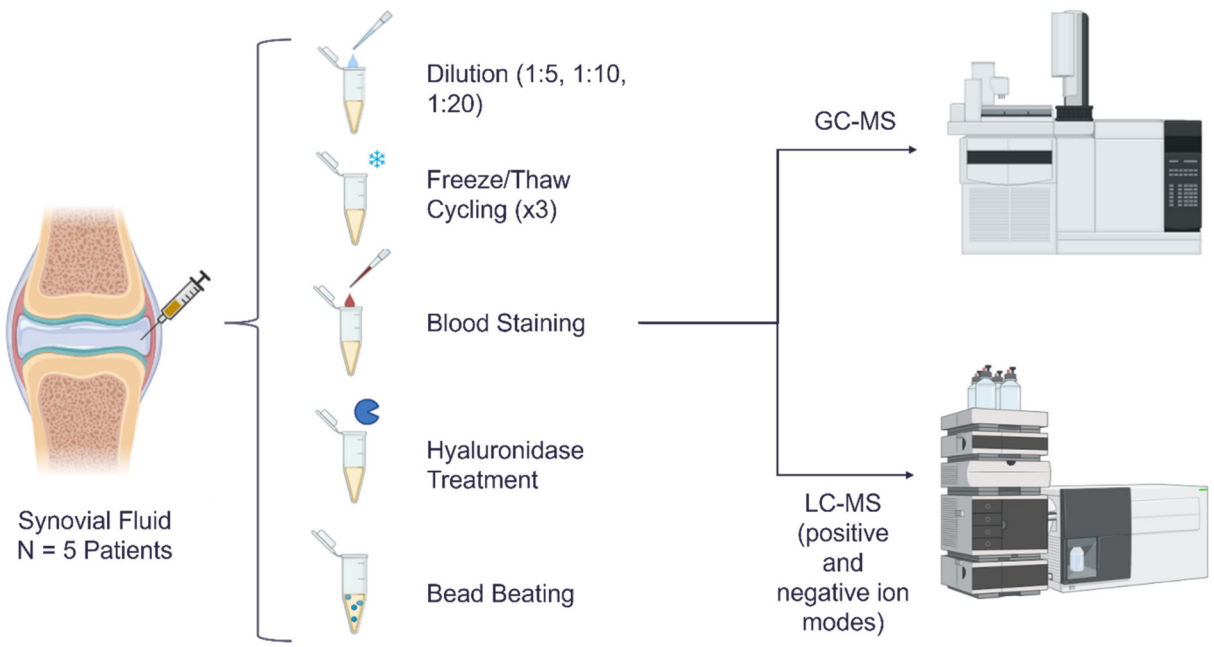

Fig. 1 Summary of the workflow applied in the current study. SF samples obtained from the knee joint were exposed to either sample dilution (1 : 5, 1 : 10 or 1 : 20; using 0.9% physiological saline), freeze–thaw cycling (up to 3 cycles), artificial blood staining using patient matched blood, and viscosity reduction *via* either enzymatic treatment with hyaluronidase or mechanical bead beating. Samples were then analysed using GC-Tof-MS for the identification of polar metabolites and UHPLC-MS (ESI+ and ESI−) for polar and non-polar metabolite identification.

This journal is © The Royal Society of Chemistry 2026

Open Access Article. Published on 21 January 2026. Downloaded on 2/26/2026 9:07:48 AM. This article is licensed under a Creative Commons Attribution-NonCommercial 3.0 Unported Licence.

GC-ToF-MS; quenching, extraction and derivatisation

Methods were adapted from Dunn *et al.*[41] Briefly, SF samples were thawed on ice and gently swirled for 10 s to homogenise the sample before aliquoting 50 μL into a 2 mL Eppendorf tube. An aliquot (50 μL) from each sample was also taken and pooled to make a quality control (QC) sample to ensure analytical robustness and reproducibility of the data during and post-analysis. Extraction blanks were also prepared according to the full extraction and derivatisation workflow.

Deproteinisation of the samples was achieved by adding 150 μL of ice-cold acetonitrile/methanol (1 : 1) and vortexing of the sample at maximum speed for 10 s. Samples were then centrifuged at 13 500*g* for 15 min following which the supernatant was collected. Samples undergoing bead beating were then transferred to vials and subjected to bead beating following which the supernatant was collected. 50 μL of internal standard solution (IS) (1.67 mg mL^{-1} of each lysine-d_4, glycine-d_5 and succinic acid-d_4 in water) was added to each sample. Samples were lyophilised in a vacuum centrifuge (Savant SpeedVac, SPD130DLX, Savant vapor trap RVT5105, Fisher Scientific, Loughborough, UK) at ambient temperature for 12 h for solvent removal.

Derivatisation of the samples was carried out by the addition of 50 μL *O*-methoxyamine-HCl in pyridine. Samples were vortexed for 10 s before being incubated at 65 °C for 40 min. 50 μL of *N*-methyl-*N*-trimethylsilyl tri fluoroacetamide (MSTFA) was then added to each sample and vortexed for 10 s before further incubation at 65 °C for 40 min. Samples were then centrifuged at 13 500*g* for 15 min following which 70 μL of the supernatant was collected and transferred to sterile GC glass vials capped with rubber sealed vial caps.

The analysis sequence was led by an extraction blank (50 μL) injection followed by an injection of a retention index (RI) sample (0.3 mg mL^{-1} of decane, dodecane, pentadecane, nonadecane and docosane in pyridine). This was then followed by six injections of the QC sample to condition the GC column and then every five sample injections were bracketed by one QC injection. Samples were randomly organised between each QC set. The run was ended by another RI sample injection as previously described by Dunn *et al.*[41] Data were collected using an Agilent GC/Q-TOF system with 280 °C inlet temperature, HP-5ms (30 m × 0.25 mm × 0.25 μm) capillary column (Agilent, Cheadle, UK), oven temperature gradient 70 °C, 4 min hold, 20 °C min^{-1} to 300 °C, 4 min hold, 300 °C transfer line temperature. Samples were run with a helium carrier gas flow rate of 1 mL min^{-1} in a constant flow mode.

GC-ToF-MS data processing and deconvolution

Data were first converted from raw vendor format into mzML format using ProteoWizard MSConvert v3 software. All raw data was deconvoluted, aligned and blank subtracted using MSDIAL v4.93 software. Results were then filtered to remove data close to the noise and deconvoluted features were assigned putative identifications *via* the matching of fragment spectra and assigned retention index with internal Centre for Metabolomics Research (CMR), Golm Metabolome 2011, NIST20 and Fiehn 2013 libraries with a retention index tolerance of 20 and electron ionisation (EI) spectral similarity cut off of 70%. Results were normalised using QC based LOESS signal correction method.[41] Data were exported from MS-DIAL into a tabular matrix containing peak annotations, retention time, assigned retention index and peak area for statistical analysis.

Ultra high performance liquid chromatography-mass spectrometry (UHPLC-MS) analysis

For extraction, samples (contained in 2 mL Eppendorf tubes) were thawed on ice and gently swirled to homogenise before adding 983 μL of 2 : 1.8 v/v LC-MS grade MeOH/H_2O (−48 °C) and vortexed for 10 s. 517 μL of LC-MS grade $CHCl_3$ was then added and samples were vortexed for 1 min before centrifugation. Where appropriate, samples underwent bead beating at this point following which the supernatant was collected in Eppendorf tubes. All samples were centrifuged for 15 min at 17 000*g* at 4 °C. Following phase separation, defined aliquots were taken from each layer prior to drying: 300 μL from the lipid (organic) phase, 600 μL from the polar (aqueous) phase, and, due to lower recovery, 100 μL from the lipid phase of bead-beaten samples, avoiding the uptake of any sediment from the interphase. These aliquots were transferred to separate 2 mL Eppendorf tubes and dried overnight in a vacuum centrifuge (Scan Speed 40 Vacuum Concentrator, Labogene) at ambient temperature for solvent removal, prior to being placed in a −80 °C freezer for storage until analysis. Extraction blanks were prepared and processed according to the full extraction workflow.

Prior to UHPLC–MS analysis, all samples were reconstituted in 150 μL of the appropriate starting solvent on ice, as detailed in the UHPLC–MS assay descriptions below. Following reconstitution, samples were vortexed for 30 s followed by centrifugation (17 000*g*, 4 °C, 15 min). From each sample, 40 μL was then transferred into two sterile 300 μL insert glass vials. A pooled QC sample was then created by aliquoting 40 μL from each sample to monitor instrument variability. Due to the low recovery volume for samples following bead beating, only 100 μL could be recovered from the lipid phase samples that were subjected to bead beating, therefore following reconstitution 30 μL of the lipid phase was transferred to four sterile 300 μL insert glass vials with a further 30 μL being used for the pool QC. All samples were analysed separately in positive and negative ion modes using a Q Exactive Quadrupole-Orbitrap instrument (Thermo Scientific) in conjunction with a Vanquish UHPLC system. Data were acquired at a mass resolution of 70 000 (FWHM at *m*/*z* 200), with the AGC target set at 10^6. The samples were analysed *via* two separate assays (assay 1 and assay 2). All assays were 15 min in length. Assay 1 was a lipidomic assay and assay 2 was a hydrophilic interaction chromatography (HILIC) assay. Assay 1 samples were reconstituted using 150 μL of H_2O: isopropyl alcohol (1 : 3) on ice and assay 2 samples were reconstituted in 150 μL of H_2O : Acetonitrile : Methanol (1 : 1 : 1) solution on ice. Assay 1

Open Access Article. Published on 21 January 2026. Downloaded on 2/26/2026 9:07:48 AM. This article is licensed under a Creative Commons Attribution-NonCommercial 3.0 Unported Licence.

used a Thermo Scientific Hypersil Gold 100 × 2.1 mm, 1.9 μm particle size column (part 25 002–102 130) with a gradient mobile phase flow rate of 0.4 mL min^{-1}; mobile phase A (60% acetonitrile, 10mM ammonium formate, 0.1% formic acid) and mobile phase B (85.5% IPA, 9.5% ACN, 5% water, 10mM ammonium formate, 0.1% formic acid). The 15 min gradient applied was as follows: 0 min, 20% B; 1.6 min, 20% B; 9.4 min, 100% B; 10.6 min, 100% B; 12.6 min, 20% B; 15 min, 20% B. An injection volume of 4 μL and a *m*/*z* range of 150–2000 Da was applied.

Assay 2 used a Thermo Scientific Accucore-150-Amide-HILIC 100 × 2.1 mm, 2.6 μm particle size column (part 16 726–102 130) with a flow rate of 0.5 mL min^{-1} and two mobile phases; mobile phase A (positive ion mode: 95% ACN, 10 mM ammonium formate, 0.1% formic acid; negative ion mode: 95% ACN, 10 mM ammonium acetate, 0.1% acetic acid) and mobile phase B (positive ion mode: 50% ACN, 10 mM ammonium formate, 0.1% formic acid; negative ion mode: 50% ACN, 10 mM ammonium acetate, 0.1% acetic acid). The 15 min gradient applied was as follows: 0 min, 20% B; 1.6 min, 20% B; 9.4 min, 100% B; 10.6 min, 100% B; 12.6 min, 20% B; 15 min, 20% B. An injection volume of 4 μL and a *m*/*z* range of 150–2000 Da was applied. Within an assay, the sample injection was randomised, with QC injections made after every fifth sample injection. Each run started with a solvent blank injection followed by three QC injections followed by an extraction blank injection then an additional 7 QC injections. Runs were terminated with a QC injection followed by an extraction blank injection.

UHPLC-MS data processing and metabolite annotation

Raw data processing was carried out using Compound Discoverer v3.3SP3. Features were identified against ThermoFisher Scientific 'mzCloud' spectral library with a score higher than 70% (MSI 2) or against in-house spectral library with score higher than 75% (MSI 1) using MSI levels reported in Sumner *et al.*[42]

Statistical analysis

Statistical analysis was carried out using MetaboAnalyst v6.0 (https://www.metaboanalyst.ca/). Metabolite features were filtered based on their relative standard deviation (RSD) values in the pooled QC samples. Metabolite features with a value above 30% were removed. Data were log_{10}-transformed to normally distribute it for univariate and multivariate statistical analysis. Autoscaling was applied for multivariate analysis only. Principal component analysis (PCA) was carried out to reduce dimensionality of the data and observe the overall trends as well as quality check the data to look at QC clustering/batch effects. The significance value was set to 0.05. Univariate analysis was carried out (*T*-test) whilst accounting for the false discovery rate (FDR) (0.05). ANOVA statistical analysis with Tukey HSD *post-hoc* analysis and linear mixed models was also carried out. A fold change (FC) threshold of 1.0 was applied and an alpha value of 0.05. Additionally, an effect-size summary was generated to quantify the number of metabolites exhibiting $a > \pm 30\%$ change in abundance relative to the control group. To evaluate linearity of the instrument response, metabolite intensities across the dilution series (1 : 5, 1 : 10, 1 : 20) were compared to expected dilution factors. For each metabolite, log_{10} intensity was regressed against log_{10} dilution factor to obtain an R^2 measure of linearity. Mean observed log_2 fold changes were also plotted against expected values, and representative metabolite response curves were generated with theoretical linear fits (SI Fig. S2).

Results

The complete metabolomics dataset is available through the MetaboLights repository, and was used for all subsequent analyses presented below.

Treatment effect on detectable metabolite numbers/classes

A total of 334 metabolite features were detected in the control group when samples were analysed using GC-MS. LC-MS/MS analysis of the control group identified a total of 1675 metabolite features in the Lipid ESI+ analysis, 833 in the Lipid ESI− mode, 763 in the HILIC ESI+ mode and 542 in the HILIC ESI− mode.

GC-ToF-MS analysis

PCA was performed to visualise overall variation between treatment groups following GC-ToF-MS analysis (Fig. 2). For the dilution, freeze–thaw, and blood staining treatments (Fig. 2A), the first two components explained 26.1% (PC1) and 12.7% (PC2) of the total variance. For the bead beating and hyaluronidase treated groups (Fig. 2B), PC1 and PC2 accounted for 54.1% and 13.9% of the total variance, respectively. Although clear group separation was not observed, slight trends in sample clustering were evident between some treatments, while QC samples formed a tight cluster in both models, indicating strong analytical reproducibility and minimal technical variation. When comparing the total numbers of metabolites detected between the control and treatment groups this was found not to be significant between the control and freeze–thaw cycling groups (2× freeze–thaw = 350, $p = 0.76$ and 3× freeze–thaw = 331, $p = 0.55$, *T*-Test) suggesting that up to three freeze–thaw cycles did not impact the detectable number of metabolites using GC-ToF-MS. However, seven metabolite classes (diazines, dioxanes, glycerolipids, phenol ethers, phenylpropanoic acids, steroids and steroid derivatives and triazolopyridazines) were observed in the 2× freeze–thaw and six (alkyl halides, epoxides, glycerolipids, oxepanes, steroids and steroid derivatives and thiophenols) in the 3× freeze–thaw groups were absent in the control group (Table 1).

A significant decrease was observed in the total numbers of metabolites detected between the control group and the three dilution groups; control = 334, 1 : 5 = 206 ($p = 0.027$), 1 : 10 = 201 ($p = 0.016$) and 1 : 20 ($p = 0.005$). Additionally, the dilution of samples resulted in the notable loss of nine metabolite classes when compared to the control group. These classes

 This journal is © The Royal Society of Chemistry 2026

Open Access Article. Published on 21 January 2026. Downloaded on 2/26/2026 9:07:48 AM.
This article is licensed under a Creative Commons Attribution-NonCommercial 3.0 Unported Licence.

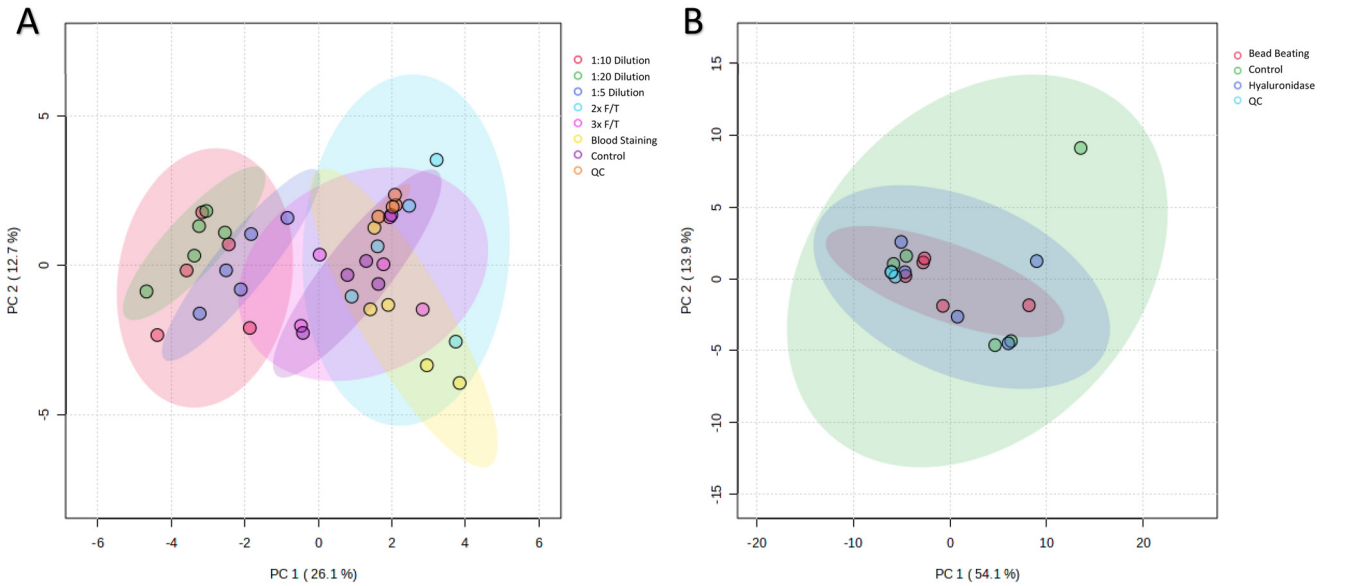

Fig. 2 PCA scores plots of GC-ToF-MS analysis. A: Plot representing dilution, freeze–thaw cycling, and blood staining treatment results, B: Plot representing bead beating and hyaluronidase treatment result. Each point represents a sample within a treatment group; A: control (purple), 1 : 5 dilution (dark blue), 1 : 10 dilution (red), 1 : 20 dilution (green), 2× freeze–thaw (light blue), 3× freeze–thaw (pink), blood stained (yellow) and B: control (green), hyaluronidase treated (blue), bead beating (red). Ellipses represent 95% confidence intervals for each group. QC samples (A: peach and B: light blue) form a tight cluster in all plots, indicating strong technical reproducibility and minimal analytical variation across runs.

were azoles, keto acids and derivatives, saturated hydrocarbons, piperidines, organic disulphides, azolidines, quinolines and derivatives, naphthalene's and furans (Table 1).

Blood staining did not result in significant changes in the total numbers of metabolites detected with 369 metabolites detected ($p = 0.94$). The identified metabolite classes, however, were altered with the identification of eight metabolite classes present in the blood staining group but absent in the control group. These include azolines, diazanaphthalenes, diazines, dithiols, halogen organides, phenol ethers, steroids/steroid derivatives and thioureas (Table 1). Pre-treatment of SF with hyaluronidase did not result in significant changes in the total numbers of metabolites detected. However, additional metabolite classes were detected in the hyaluronidase treated group compared to the control group. These were: azolines, benzothiophenes, diazanaphthalenes, diazines, homogeneous alkali metal compounds, organic carbonic acids and derivatives, oxepanes, phenols and phenol ethers, steroids and steroid derivatives and thioureas (Table 1). Hyaluronidase treatment also resulted in the lack of identification of other classes detected in the control group which were: indoles and derivatives, naphthalenes, organic disulfides and prenol lipids.

GC-ToF-MS analysis revealed bead beating to significantly reduce the numbers of detectable metabolites (total numbers of metabolites detected; control = 230; bead beating = 176; $p = 1.15 \times 10^{-9}$). Metabolite class analysis revealed metabolite classes including amino acids and derivatives, sterols and hormones, siloxanes and derivatives and aromatic and heterocyclic compounds to be absent from the bead beating group. However, there was no clear separation between the bead beating group and the control group in the PCA analysis (Fig. 2B).

UHPLC-MS analysis

For the group of samples that underwent bead beating, a significant increase in the number of detectable metabolites was discerned in lipid reversed phase LC-MS ESI+ mode (1743, $p = 1.28 \times 10^{-5}$) compared to control (1675). No significant change was observed in the lipid ESI− mode or HILIC analysis. PCA of the lipid ESI+ mode data revealed clear separation and clustering of the bead beating group to other treatments groups with components 1 and 2 accounting for 26.2% and 12.6% of the total variation respectively (Fig. 3A). However, no clear separation is observed in the lipid ESI− PCA plot (Fig. 3B) with the first two components explaining 76.2% (PC1) and 4.8% (PC2) of total variance.

No significant changes in total detectable numbers were observed in the samples that underwent freeze–thaw cycling in both lipid and HILIC analysis compared to control. Moreover, no significant changes were observed in the total numbers of detectable metabolites between the control group and the hyaluronidase treated group in both lipid and HILIC analysis.

Sample dilution demonstrated significant changes across both HILIC and lipid analysis; by which the total number of metabolites observed significantly decreased with increasing dilution. A total of 763 metabolite features were detected in the HILIC ESI+ mode and 542 in the ESI− mode, for undiluted samples. These decreased to 680 (1 : 5 dilution, $p = 5.03 \times 10^{-11}$), 636 (1 : 10 dilution, $p = 1.69 \times 10^{-20}$) and 565 (1 : 20

Open Access Article. Published on 21 January 2026. Downloaded on 2/26/2026 9:07:48 AM. This article is licensed under a Creative Commons Attribution-NonCommercial 3.0 Unported Licence.

Table 1 The table highlights the metabolite classes identified in the data set and the number of identified metabolites per metabolite class in each treatment group. Metabolites were identified at identified at MSI level 2 confidence level (GC-ToF-MS)

Chemical class	Control	1 : 5 dilution	1 : 10 dilution	1 : 20 dilution	2× freeze–thaw	3× freeze–thaw	Blood staining	Hyaluronidase treatment	Bead beating
Alkyl halides	0	1	0	0	0	1	0	0	1
Anthracenes	0	0	0	0	0	0	0	0	1
Azoles	2	0	0	0	1	0	1	1	1
Azolidines	1	0	0	0	0	0	0	0	0
Azolines	0	0	0	0	0	0	1	1	0
Benzene and substituted derivatives	10	7	3	3	10	8	7	6	2
Benzothiophenes	0	0	0	0	0	0	1	1	0
Benzotriazoles	1	1	1	0	1	1	1	1	0
Carboxylic acids and derivatives	30	18	13	8	27	28	34	34	14
Diazanaphthalenes	0	0	0	0	0	0	1	1	1
Diazines	0	1	1	1	1	0	1	1	0
Dihydrofurans	1	1	1	1	1	1	1	1	0
Dioxanes	0	0	0	0	1	0	0	0	0
Dithioles	0	0	0	0	0	0	1	0	0
Epoxides	0	0	0	0	0	1	0	0	0
Fatty Acyls	7	2	1	3	9	11	11	11	1
Furans	1	0	0	0	1	1	1	1	0
Glycerolipids	0	0	0	0	1	1	0	0	0
Halogen organides	0	1	1	0	0	0	1	0	0
Homogeneous alkali metal compounds	0	0	0	0	0	0	0	1	0
Hydroxy acids and derivatives	5	1	1	1	3	3	3	3	3
Imidazopyrimidines	4	2	2	2	4	4	4	4	2
Indanes	0	0	0	0	0	1	0	0	0
Indoles and derivatives	2	0	1	1	1	0	1	0	2
Keto acids and derivatives	4	0	0	0	4	5	3	5	3
Lactones	3	2	4	1	3	2	4	4	1
Naphthalenes	1	0	0	0	0	0	0	0	0
Organic carbonic acids and derivatives	0	0	0	0	0	0	0	1	0
Organic disulfides	1	0	0	0	0	0	0	0	0
Organic phosphoric acids and derivatives	1	1	0	1	1	1	1	1	0
Organometalloid compounds	2	6	4	2	6	3	5	3	8
Organonitrogen compounds	3	0	0	2	3	3	2	2	0
Organooxygen compounds	25	14	18	14	22	18	30	30	12
Oxazinanes	1	1	1	1	1	1	1	1	0
Oxepanes	0	1	1	1	0	1	0	1	0
Phenethylamines	0	0	0	0	0	0	0	0	0
Phenol ethers	0	0	0	0	2	2	1	1	0
Phenols	0	0	0	0	0	0	0	1	1
Phenylpropanoic acids	0	0	0	0	1	0	0	0	0
Piperidines	3	0	0	0	3	1	2	2	1
Prenol lipids	1	0	0	0	2	2	0	0	0
Pyridines and derivatives	1	1	0	0	2	2	2	2	0
Quinolines and derivatives	1	0	0	0	0	0	1	1	1
Saturated hydrocarbons	1	0	0	0	0	1	0	0	1
Steroids and steroid derivatives	0	0	0	0	2	2	1	1	0
Thiophenols	0	0	1	0	0	1	0	0	0
Thioureas	0	0	0	1	0	0	1	1	0
Triazolopyridazines	0	0	0	0	1	0	0	0	0
Unsaturated hydrocarbons	0	0	0	0	0	0	0	0	1

dilution, $p = 2.29 \times 10^{-39}$) in the ESI+ mode and 415 (1 : 5 dilution, $p = 4.23 \times 10^{-25}$), 376 (1 : 10 dilution, $p = 6.16 \times 10^{-37}$), 329 (1 : 20 dilution, $p = 3.38 \times 10^{-53}$) in the ESI− mode. 1675 and 833 metabolites were detected in the lipid analysis control group in ESI+ and ESI− modes respectively. These totals decreased to 1532 (1 : 5 dilution, $p = 1.43 \times 10^{-12}$), 1366 (1 : 10 dilution, $p = 1.04 \times 10^{-42}$) and 1276 (1 : 20 dilution, $p = 4.60 \times 10^{-64}$) in the ESI+ mode and 753 (1 : 5 dilution, $p = 4.20$

This journal is © The Royal Society of Chemistry 2026

Open Access Article. Published on 21 January 2026. Downloaded on 2/26/2026 9:07:48 AM.
This article is licensed under a Creative Commons Attribution-NonCommercial 3.0 Unported Licence.

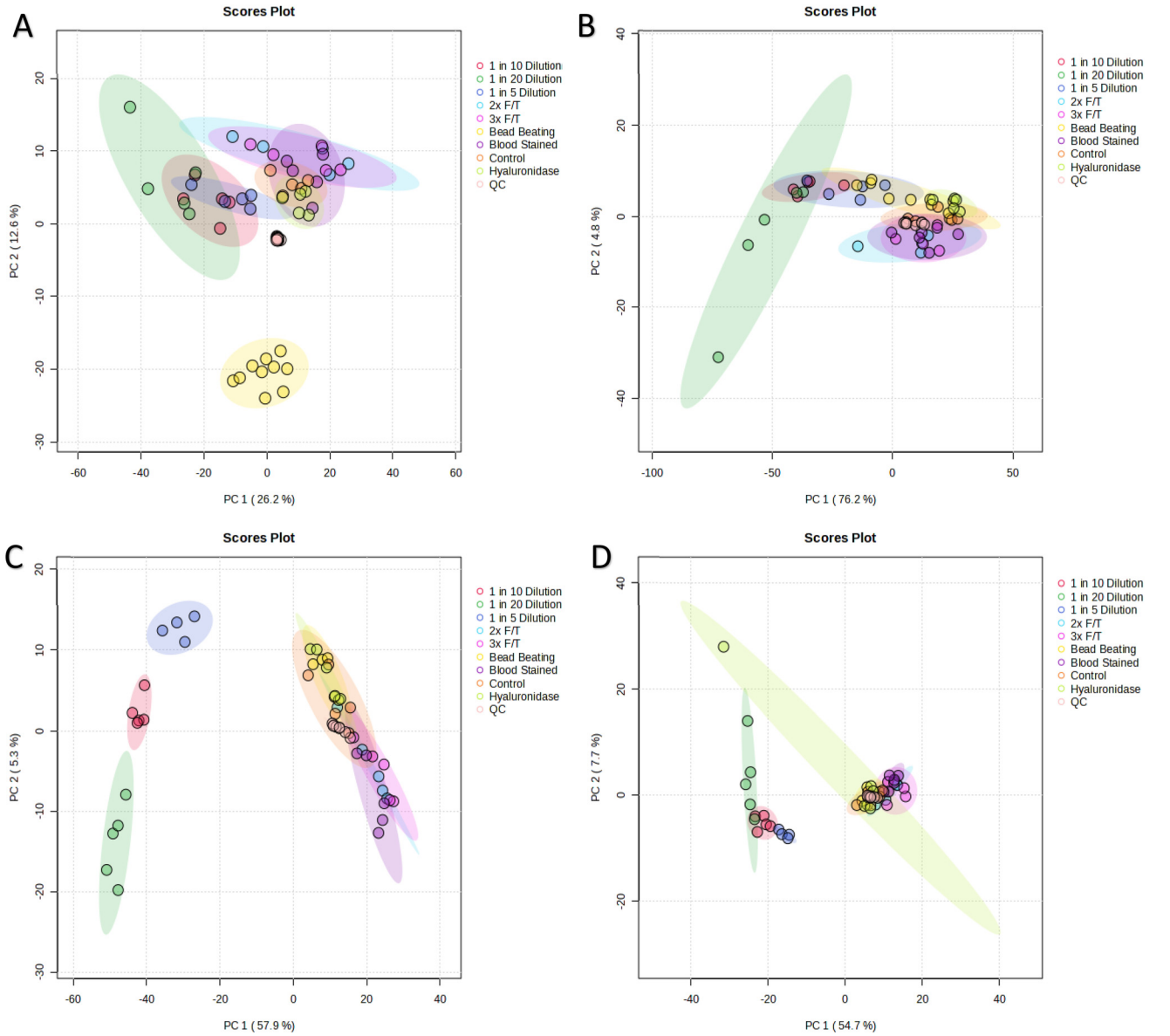

Fig. 3 PCA scores plots of the UHPLC-MS Lipid and HILIC analysis following different treatments. Each point represents an individual sample within a treatment group; control (orange), 1 : 5 dilution (dark blue), 1 : 10 dilution (red), 1 : 20 dilution (dark green), 2× freeze–thaw (light blue), 3× freeze–thaw (pink), blood stained (purple), hyaluronidase treated (light green), bead beating (yellow). Ellipses represent 95% confidence intervals for each group. QC samples (peach) form a tight cluster in all plots, indicating strong technical reproducibility and minimal analytical variation across runs. A: UHPLC-MS Lipid ESI+, B: UHPLC-MS Lipid ESI–, C: UHPLC-MS HILIC ESI+, D: UHPLC-MS HILIC ESI–.

$\times 10^{-20}$), 618 (1 : 10 dilution, $p = 2.08 \times 10^{-64}$) and 508 (1 : 20 dilution, $p = 8.60 \times 10^{-107}$) in the ESI– mode. PCA scores plots of these data demonstrated clear separation amongst the three dilution groups in the HILIC ESI+ analysis (Fig. 3C) with no overlap of the 95% confidence intervals. Components 1 and 2 of the PCA explained 57.9% and 5.3% of total variance in the HILIC ESI+ mode (Fig. 3C) and 54.7% and 7.7% in the HILIC ESI– mode (Fig. 3D).

UHPLC-MS HILIC analysis demonstrated a significant increase in the number of metabolite features detected by ESI– mode for samples in the blood staining group ($n = 557$) compared to the control samples ($n = 542$) ($p = 0.04$). Conversely a significant decrease in the number of compounds was discerned in lipid ESI– mode in the blood staining group *vs.* control (823 and 833 respectively; $p = 0.05$). By further contrast, no significant changes were apparent in the HILIC ESI+ nor lipid ESI+ in observed compounds between the blood stained and control sample groups.

Treatment effect on relative metabolite abundances: GC-ToF-MS analysis

The analysis showed that relative metabolite abundances varied significantly between different metabolites within the same subject ($p < 2 \times 10^{-16}$), indicating substantial differences

Open Access Article. Published on 21 January 2026. Downloaded on 2/26/2026 9:07:48 AM. This article is licensed under a Creative Commons Attribution-NonCommercial 3.0 Unported Licence.

Table 2 Differential abundance (≥±2 $\log_2$ fold change; $p < 0.05$) of metabolites that were identifiable (MSI level 2 confidence) across SF treatment conditions

Contrast	$\log_2$ fold change	*P*-Value	Metabolite name
1 : 5 dilution – control	0.9534	0.8	Octahydroindolizine
1 : 10 dilution – control	2.569	0.00	Octahydroindolizine
1 : 20 dilution – control	1.595	0.18	Octahydroindolizine
2× F/T – control	2.329	0.01	Octahydroindolizine
3× F/T – control	1.286	0.45	Octahydroindolizine
Blood stain – control	1.051	0.70	Octahydroindolizine
Hyaluronidase – control	3.699	0.00	Octahydroindolizine
Blood stain – control	2.678	0.00	4-Fluoro-DL-tryptophan

in their levels. Treatment effects within subjects were also highly significant ($p < 2 \times 10^{-16}$), as was the interaction between treatment and metabolite ($p < 2 \times 10^{-16}$) demonstrating a clear treatment effect beyond baseline variability. Subsequent fold change analysis identified two metabolites that exhibited increased relative abundance across all groups, excluding the bead beating group compared to the control. One of the metabolites was identified as octahydroindolizine ($C_{17}H_{23}N$) at MSI level 2 confidence level through accurate mass and RI matching (Table 1) though the second remains unidentified. Additionally, four metabolites showed increased fold change specifically in the blood-stained treatment group; among these, one was identified as 4-fluoro-DL-tryptophan that had a significant $\log_2$ FC of 2.678 ($p < 0.00$) (Table 2).

Treatment effect on relative metabolite abundances: UHPLC-MS analysis

To assess this effect on the UHPLC-MS data, the data were fitted against a linear mixed model using patient ID as a random effect and treatment as a fixed effect. This model tested the overall (omnibus) impact of treatment across all metabolites within each assay and polarity. The lipid (ESI+ and ESI–) and HILIC (ESI+) results demonstrated that treatment had a significant impact on metabolite abundances (lipid ESI+; $p = 8.17 \times 10^{-10}$, lipid ESI–; $p = 5.05 \times 10^{-13}$, HILIC ESI+: $p = 2.04 \times 10^{-6}$), however results for HILIC ESI– were not significant ($p = 0.93$). These p-values reflect global tests of treatment effects across all metabolites, not per-feature significance levels. Treatment *via* sample dilution had the greatest effect on metabolite abundances (Table 3) resulting in a significant decrease in relative metabolite abundances (Lipid ESI+/ESI– and HILIC ESI+).

Table 3 Impact of sample dilution on metabolite abundance across UHPLC-MS Lipid and HILIC analyses. *P* values from statistical comparisons (relative to control) are shown for each dilution level (1 : 5, 1 : 10, 1 : 20) across three analytical methods: Lipid ESI+, Lipid ESI– and HILIC ESI+. Samples dilution resulted in significant reductions ($p < 0.05$) across all three analytical platforms

Analysis	Treatment	*P*-Value
RP LC-MS Lipid ESI+	1 : 5 dilution	9.27×10^{-4}
	1 : 10 dilution	1.65×10^{-4}
	1 : 20 dilution	9.16×10^{-5}
RP LC-MS Lipid ESI–	1 : 5 dilution	4.2×10^{-4}
	1 : 10 dilution	5.73×10^{-5}
	1 : 20 dilution	2.30×10^{-5}
HILIC-MS ESI+	1 : 5 dilution	0.05
	1 : 10 dilution	0.02
	1 : 20 dilution	0.02

Linearity of dilution

To assess whether signal intensity scaled linearly with sample dilution, the relationship between measured abundance and expected dilution factor was evaluated for both analytical techniques (SI Fig. S6–S9). Mean observed $\log_2$ fold changes deviated from the theoretical 1 : 1 response, particularly in the HILIC ESI^+ mode. The distribution of R^2 values revealed that most metabolites exhibited sub-linear behaviour ($R^2 < 0.9$), consistent with matrix-dependent ion suppression. Representative metabolite response curves further illustrated the flattening of slopes at higher dilutions, supporting the conclusion that non-linear detector response contributes to the observed loss of features with dilution.

Lipid analysis

Lipid analysis using reversed phase (RP) LC-MS in the ESI+ mode revealed 37 metabolite features that had an increased abundance in the bead beating group compared to the control group, as demonstrated by an increase in their fold change (Fig. 4A). These compounds formed a coherent cluster suggesting a shared response to the mechanical disruption. Though not all compounds could be reference matched to spectral libraries, those that were matched (Table 4) could be broken down into the several classes: prenol lipids, benzothiazines glycerolipids, indoles and derivatives, carboxylic acids and derivatives, quinolines and derivatives and dioxanes. Additionally, the apparent clustering of the data in the PCA plots revealed there to be low overlap between the metabolites in the bead beating group *versus* other treatment groups, thus highlighting the unique extraction profile produced by this treatment.

In contrast however, the three dilution groups demonstrate a pronounced decrease in fold change in the metabolite abundances of 13 metabolites (dark blue) (Fig. 4A). An increase in the metabolite abundance of four metabolites (red) across all three dilution groups was observed compared to control. These metabolites are currently unidentified. Two metabolites that showed consistent decrease in fold change across the 2× Freeze–thaw, bead beating and blood staining treatment groups, as well as two metabolites with an increased relative abundance in the blood staining group (Fig. 4B) similarly remain unannotated.

HILIC analysis

Fold change analysis revealed sample dilution to decrease the relative abundances of metabolites in both ESI+ and ESI– modes. By contrast, results revealed metabolites demonstrating a significant increase in relative abundance in the blood staining group compared to control; these were identified as ethylenediaminetetraacetic acid (EDTA) (FC: 6.76, $p = 1.00 \times 10^{-15}$) (ESI+), hypoxanthine (FC: 4.9, $p = 6.22 \times 10^{-09}$) and

This journal is © The Royal Society of Chemistry 2026

Open Access Article. Published on 21 January 2026. Downloaded on 2/26/2026 9:07:48 AM.
This article is licensed under a Creative Commons Attribution-NonCommercial 3.0 Unported Licence.

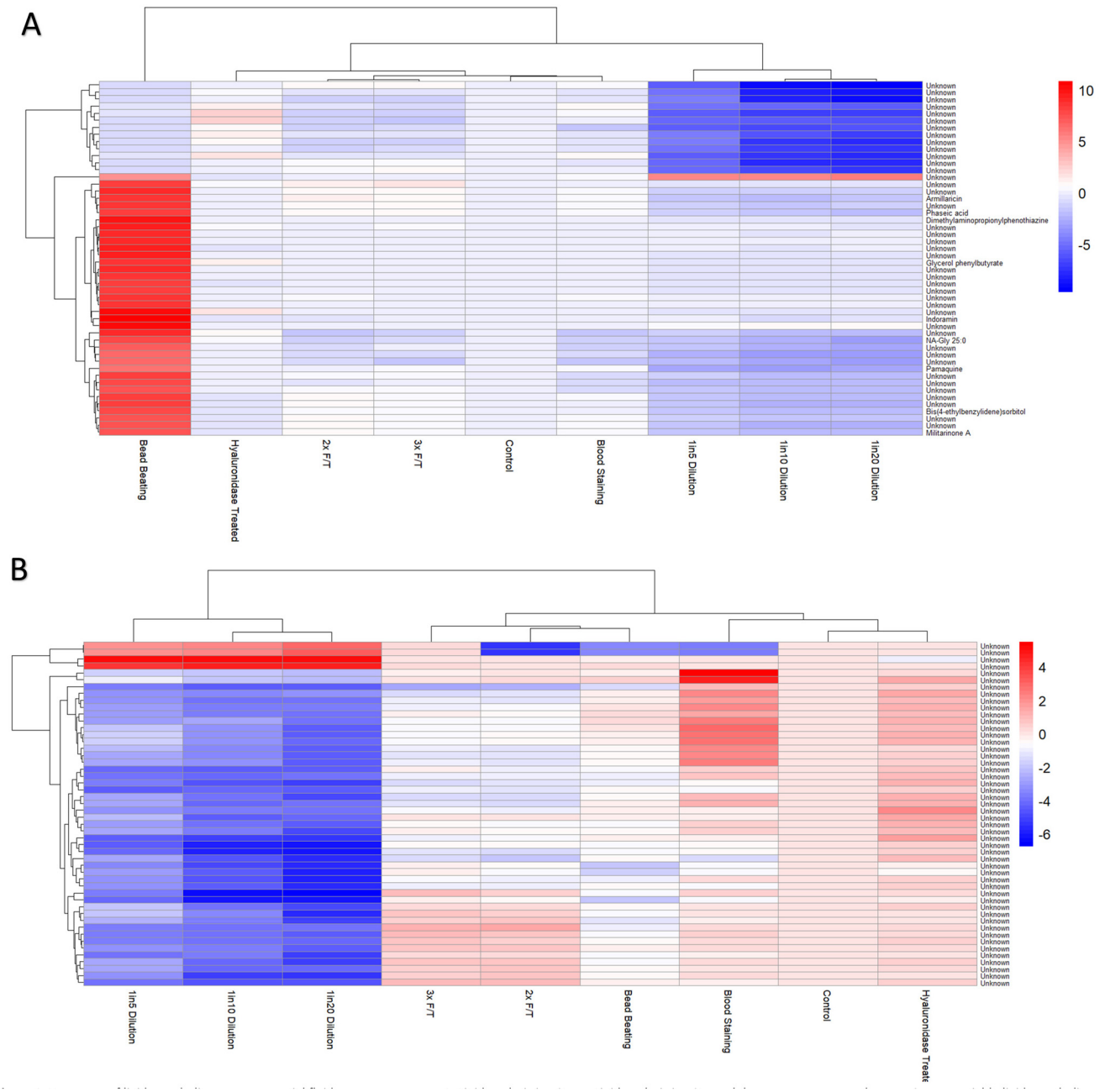

Fig. 4 Heatmaps of lipid metabolites across synovial fluid treatment groups. A: Lipid analysis in ESI+. B: Lipid analysis in ESI−. Each heatmap represents the top 50 most variable lipid metabolites in each treatment group. Values represent $\log_2$ fold changes in metabolite abundance relative to control group, calculated per metabolite. Columns represent individual treatments and rows correspond to individual lipid metabolites. Red indicates a higher abundance and blue a lower abundance relative to control. Hierarchical clustering reveals distinct shifts in lipid profiles driven by treatment effects.

adenine (FC: 6.9, $p = 3.44 \times 10^{-10}$) (ESI−) (MS2 confidence level). One metabolite demonstrated as highly abundant in the bead beating group in both ESI+ (FC: 9.98, $p = 1.00 \times 10^{-15}$) and ESI− (FC: 6.97, $p = 1.00 \times 10^{-15}$) modes was identified as 1*H*-Indol-3-ylamine (MS2 confidence level). Also identified amongst the metabolites that demonstrated a trend towards decreased relative abundance in the bead beating and hyaluronidase treated groups compared to the control (ESI+) though not significant 1-palmitoyl-2-linoleoyl-*sn-glycero*-3-PC (FC: −5.69, $p = 0.74$ and FC: 2.07, $p = 0.77$ respectively).

Discussion

These findings collectively suggest that not only do SF acquisition techniques and pre-treatments strongly influence

Open Access Article. Published on 21 January 2026. Downloaded on 2/26/2026 9:07:48 AM. This article is licensed under a Creative Commons Attribution-NonCommercial 3.0 Unported Licence.

Table 4 Metabolites significantly enriched in synovial fluid following bead beating treatment (Lipid ESI+). The table lists metabolites demonstrating a significant increase in abundance relative to control as detected by UHPLC-MS Lipid ESI+. All metabolites were identified at MSI level 2 confidence level

Contrast	Log_2 fold change	*P*-Value	Metabolite name
Bead beating – control	8.68	2.55×10^{-5}	Armillaricin
Bead beating – control	8.18	4.47×10^{-9}	Phaseic acid
Bead beating – control	10	7.44×10^{-4}	Dimethylaminopropionylphenothiazine
Bead beating – control	8.69	3.87×10^{-7}	Glycerol phenylbutyrate
Bead beating – control	10.84	1.03×10^{-7}	Indoramin
Bead beating – control	7.97	6.93×10^{-6}	NA-Gly 25:0
Bead beating – control	5.95	2.83×10^{-6}	Pamaquine
Bead beating – control	7.77	7.85×10^{-9}	Bis(4-ethylbenzylidene)sorbitol
Bead beating – control	7.25	2.24×10^{-11}	Militarinone A

metabolite concentrations, but that the magnitude and direction of the treatment effect differs between individual metabolites.

Although SF is normally yellow-straw colour, blood contamination is occasionally observed in clinical samples. Traumatic arthrocentesis, in which a small blood vessel is punctured during aspiration, is the most common cause, while inflammation or joint trauma can also increase vascular permeability and introduce red blood cells (RBCs) into the joint space. In such cases, visible red discoloration of the fluid may persist even after centrifugation, indicating that red cells have lysed and released haemoglobin and intracellular metabolites into the SF. The resulting alterations represent haemolytic contamination, a clinically relevant pre-analytical artifact that can occur in real-world SF sampling when aspiration is difficult or processing is delayed. Once haemolysis occurs, centrifugation cannot reverse the release of intracellular metabolites or haemoglobin. These observations highlight the importance of careful aspiration technique, prompt sample separation, and visual inspection of SF colour prior to metabolomic analysis.

The identification of highly abundant metabolite features in the blood staining group across both GC-ToF-MS and UHPLC-MS (HILIC) analysis demonstrate the significant influence of blood derived – particularly polar molecules – on the SF metabolomic profile. Notably, 4-fluoro-DL-tryptophan was elevated in blood-stained samples which may reflect plasma-derived contamination or haemolysis-related metabolic shifts.[43] Adenine and hypoxanthine were also among the abundant metabolite features identified. Adenine is a precursor to adenine nucleotides such as ATP whilst hypoxanthine is a purine derivative that acts as an intermediate in ATP metabolism and the formation of nucleic acids.[44] Our findings of elevated levels of adenine and hypoxanthine in the blood staining group are consistent with previous findings where an increase in the diffusion of non-phosphorylated purine metabolites from RBCs into plasma/serum post sample collection have been associated with blood temperature and prolonged plasma contact with cells.[45] A similar mechanism may occur in blood-stained SF samples, therefore further highlighting the importance of tightly controlling post-collection sample handling and selection to reduce the artefactual elevation of RBC derived metabolites in SF samples. Aside from acting as a marker of blood staining of the SF, the increased presence of hypoxanthine in SF samples can also potentially indicate towards the presence of inflammatory forms of arthritis such as gout.[46] Gout is caused by the buildup of uric acid formed through the oxidative hydroxylation of hypoxanthine to xanthine and xanthine to uric acid *via* the enzyme xanthine oxidoreductase.[47]

The presence of EDTA in this study is associated with the artificial staining of the SF using blood that was collected in EDTA tubes. This makes the EDTA a reflection of the sample collection-handling process rather than the natural state of the sample. Additionally, octahyroindolizine also known as indolizine is an exogenous, naturally occurring bicyclic compound with widespread manufacturing and pharmaceutical applications.[48] The consistent increase in octahydroindolizine across all treatment groups compared to the control group suggests it could be an artifact of sample handling. These findings provide valuable reference for best practices in future metabolomic studies. By identifying markers of blood contamination and sample handling this study highlights the importance of contamination related features that researchers should be aware of as potential confounders when interpreting metabolic profiles.

Lipid analysis using reversed phase LC-MS in ESI+ and ESI− modes demonstrates the marked impact of SF preparation on lipid abundance profiles. However, the magnitude and pattern of response varied between the two modes. In the ESI+ mode, the most marked difference in the bead beating group was observed, with widespread and strong enrichment of lipid features compared to other treatments. The majority of the putatively identified compounds have been shown to be associated with extrinsic origins including pharmaceuticals, plant and fungus derived natural products and synthetic analogues, which may have come from the diet. Bead beating is a technique commonly applied in metabolomic studies as a means of sample homogenisation and cellular disruption.[49] Previous studies applying bead beating on faecal and soft tissue samples (like liver and breast) have shown it to contribute towards the increased detection of lipid metabolites.[50–52]

The application of bead beating on SF homogenisation and matrix disruption has not been explored until now. Our find-

 This journal is © The Royal Society of Chemistry 2026

Open Access Article. Published on 21 January 2026. Downloaded on 2/26/2026 9:07:48 AM.
This article is licensed under a Creative Commons Attribution-NonCommercial 3.0 Unported Licence.

ings suggest bead beating may enhance the liberation of exogenous compounds from the sample matrix. These findings suggest that bead beating may be an effective treatment at extracting a broad range of lipid classes in the SF that ionise well in ESI+. Lipid ESI− on the other hand revealed a different pattern, with the most prominent observation being the decrease in relative FC of compounds in the three dilution groups. GC-Tof-MS analysis on the other hand suggests bead beating may impact metabolite detection, although the lack of clear separation in the PCA analysis between the bead beating and control groups suggests overall metabolite variance was dominated by shared high abundance of features such as sugars. Together these results underscore the importance of matching sample treatment strategies with the strengths of the analytical technique.

Metabolomic studies often benefit from sample dilution as excessively concentrated injections can cause column overloading, signal saturation and non-linear signal responses with features falling below the detection limit.[53] Further, in some instances where SF volume is limited (where there is a lack of effusion), sample dilution is required to retrieve any material for analysis. However, a common trend observed across all analytical methods applied in this study was the reduction in both the number and relative abundance of detectable metabolites with increasing sample dilution. The clear separation of the dilution groups demonstrated in the PCA analysis particularly in the HILIC ESI+ analysis suggests that even moderate changes in sample dilution can cause substantial shifts in metabolomic profiles and highlights its role as a source of both reproducible and systemic variation.

These results suggest that for untargeted SF analysis dilution may hinder rather than enhance metabolite coverage. As such, maintaining adequate sample concentration appears critical for achieving broad and reliable metabolite coverage independent of the analytical platform used. Moreover, where samples are differentially diluted, *e.g.* due to clinical harvest method, it is important that this dilution is accounted for before metabolomic analysis. This can be achieved *via* determining the SF dilution factor, using an established methodology in which urea is measured in patient matched SF and plasma and then samples manually diluted to align with the most dilute sample.[19] However, the data provided in this analysis provides important information about specific metabolites whose differential abundances should be interpreted with caution in the case of differential dilution.

To further explore the effect of sample dilution on analytical performance, the linearity of detector response was evaluated across the 1 : 5, 1 : 10, and 1 : 20 dilution series (SI Fig. S2 and S3). The observed mean $\log_2$ fold changes deviated from the theoretical 1 : 1 relationship, and the majority of metabolites exhibited R^2 values below 0.9, indicating a sub-linear response to dilution. Representative metabolite intensity–dilution curves further confirmed signal attenuation at higher dilutions, consistent with matrix-dependent ion suppression and reduced ionisation efficiency. Within the range tested, dilution factors between approximately 1 : 5 and 1 : 10 maintained adequate signal intensity while avoiding potential detector saturation, representing a practical balance between matrix effects and signal loss. Although ion suppression was not directly measured, this inference is supported by the sub-linear response behaviour observed across the dilution series. Together, these findings emphasise that while modest dilution can be tolerated, undiluted SF samples yield the broadest metabolite coverage and should be prioritised for untargeted workflows whenever feasible.

In this study, all datasets were normalised using QC-based LOESS correction to account for instrumental drift and analytical variability. Normalisation strategies that correct for sample-specific dilution, such as urea ratio, total metabolite or protein content normalisation, and probabilistic quotient normalisation (PQN[54]), were not applied, as the goal was to evaluate the intrinsic impact of pre-analytical sample handling. Future work to assess whether such normalisation approaches can reduce dilution-related bias in clinical SF metabolomics, where variable sample volume and viscosity are often unavoidable is required.

Freeze–thaw cycling did not demonstrate a significant impact on the total numbers of metabolites/metabolite features that were detectable across both of the analytical methods compared in this study. Additionally, clear separation of the samples that underwent freeze–thaw cycling from the rest of the treatment groups visualised on the PCA scores plots suggested minimal impact of this variable on metabolome profile. These results suggest that the SF metabolome exhibits a high level of stability for up to three freeze–thaw cycles. These results are in line with previous studies by Jaggard *et al.*[32] and Damyanovich *et al.*[30] that tested the impact of up to 5 and 10 freeze–thaw cycles respectively using nuclear magnetic resonance (NMR) where SF samples demonstrated stability with no significant changes to detectable metabolites observed.

The enzymatic treatment of SF with hyaluronidase is widely applied in proteomic studies where it has been shown to enhance the detection of proteins in addition to viscosity reduction and sample homogenisation.[31,55] However, no studies have explored its impact on enhancing SF metabolite detection. The results from this do not suggest this treatment to significantly increase the total numbers of detectable metabolites.

Though this study has provided valuable initial insights into the effects of pre-analytical variable on the SF metabolome, several limitations should be acknowledged. This study was limited by the small sample size (n = 5 per treatment group) which restricts statistical power to detect more subtle effects. Consequently, the PCA results should be interpreted qualitatively as a means of visualising general trends. Additionally, the use of artificially induced blood staining while controlled may not fully replicate the complexity of spontaneous hemarthrosis or clinical contamination scenarios. While the study investigated the impact of up to three freeze–thaw cycles, it did not explore variations in thawing conditions (*e.g.* room temperature *vs.* ice) or the impact of storage under

Open Access Article. Published on 21 January 2026. Downloaded on 2/26/2026 9:07:48 AM. This article is licensed under a Creative Commons Attribution-NonCommercial 3.0 Unported Licence.

different conditions or storage time, all of which may further influence metabolite stability. Future work should include larger cohorts to validate the findings in this study and investigate additional pre-analytical factors that were not explored in the current study. Finally, the level of metabolite identification is rarely to MSI level 1,[42] but this does not limit the findings in terms of the number metabolite features that are different between the various treatment groups.

Conclusions

This study provides methodological insights into the growing field of SF metabolomics which holds great potential for improving our understanding of joint diseases and the identification of clinically relevant biomarkers. The findings presented not only emphasise the impact of pre-analytical factors and handling on the SF metabolic profile but also highlight treatments that may be beneficial for enhancing metabolite extraction and profiling. Ultimately, refining these analytical workflows will strengthen the utility of SF in translational research and facilitate the discovery of biomarkers reflective of disease biology as opposed to pre-analytical variation.

Author contributions

Conceptualization, C. H.; methodology, Y. L., A. B., N. G., R. G., K. W., J. P., C. H.; formal analysis, Y. L., A. B., N. G., C. H.; investigation, Y. L., A. B., N. G.; resources, K. W., R. G., C. H.; data curation, Y. L., C. H.; writing – original draft preparation, Y. L.; writing – review and editing, Y. L., A. B., N. G., R. G., K. W., J. P., C. H., ; visualization, Y. L.; supervision, A. B., N. G., R. G., K. W., J. P., C. H.; project administration, Y. L., C. H..; funding acquisition, C. H. All authors have read and agreed to the published version of the manuscript.

Conflicts of interest

The authors declare no conflicts of interest.

Ethical statement

All experiments were performed in compliance with relevant laws and guidelines. Ethical approvals were obtained from the National Research Ethics Service – North West Committee (11/NW/0875). Synovial fluid and blood samples were collected from patients who had provided informed consent.

Data availability

Raw metabolomic data is available at MetaboLights repository. Any additional data will be made available upon request to the corresponding author. Supplementary information (SI) is available. See DOI: https://doi.org/10.1039/d5an00943j.

Acknowledgements

We would like to thank Keele University for funding this PhD studentship. The sponsors had no involvement in the study design, data collection and interpretation or preparation of the manuscript. This study has been delivered through the National Institute for Health and Care Research (NIHR) Birmingham Biomedical Research Centre (BRC). The views expressed are those of the author(s) and not necessarily those of Keele University, the MRC, the NIHR or the Department of Health and Social Care. For the purposes of open access, the author has applied Creative Commons Attribution (CC-BY) licence to any accepted author manuscript version arising from this submission.

References

1 J. Bolander, M. Teresita, G. Poehling, O. Jochl, E. Parsons, W. Vaughan, *et al.*, The synovial environment steers cartilage deterioration and regeneration, *Sci. Adv.*, 2023, **9**(16), eade4645, DOI: 10.1126/sciadv.ade4645.
2 M. Marian, R. Shah, B. Gashi, S. Zhang, K. Bhavnani, S. Wartzack, *et al.*, Exploring the lubrication mechanisms of synovial fluids for joint longevity – A perspective, *Colloids Surf., B*, 2021, **206**, 111926.
3 S. Kim, J. Hwang, J. Kim, S.-H. Lee, Y. E. Cheong, S. Lee, *et al.*, Metabolic discrimination of synovial fluid between rheumatoid arthritis and osteoarthritis using gas chromatography/time-of-flight mass spectrometry, *Metabolomics*, 2022, **18**(7), DOI: 10.1007/s11306-022-01893-9.
4 S. M. Mahendran, K. Oikonomopoulou, E. P. Diamandis and V. Chandran, Synovial fluid proteomics in the pursuit of arthritis mediators: An evolving field of novel biomarker discovery, *Crit. Rev. Clin. Lab. Sci.*, 2017, **54**, 495–505.
5 H. S. Jónasdóttir, H. Brouwers, J. C. Kwekkeboom, H. M. J. van der Linden, T. Huizinga, M. Kloppenburg, *et al.*, Targeted lipidomics reveals activation of resolution pathways in knee osteoarthritis in humans, *Osteoarthritis Cartilage*, 2017, **25**, 1150–1160.
6 C. J. Mathews and G. Coakley, Septic arthritis: current diagnostic and therapeutic algorithm, *Curr. Opin. Rheumatol.*, 2008, **20**, 457–462.
7 A. Bodaghi, N. Fattahi and A. Ramazani, Biomarkers: Promising and valuable tools towards diagnosis, prognosis and treatment of Covid-19 and other diseases, *Heliyon*, 2023, **9**, e13323.
8 S. W. Kong and C. Hernandez-Ferrer, Assessment of coverage for endogenous metabolites and exogenous chemical compounds using an untargeted metabolomics platform, *Pac. Symp. Biocomput.*, 2020, **25**, 587.

This journal is © The Royal Society of Chemistry 2026

Open Access Article. Published on 21 January 2026. Downloaded on 2/26/2026 9:07:48 AM. This article is licensed under a Creative Commons Attribution-NonCommercial 3.0 Unported Licence.

9 C. D. DeHaven, A. M. Evans, H. Dai and K. A. Lawton, Organization of GC/MS and LC/MS metabolomics data into chemical libraries, *J. Cheminf.*, 2010, **2**(1), 9, DOI: 10.1186/1758-2946-2-9.
10 Y. Chen, E.-M. Li and L.-Y. Xu, Guide to Metabolomics Analysis: a Bioinformatics Workflow, *Metabolites*, 2022, **12**, 357.
11 Q. Zhang, T. Zhang, H. Lv, L. Xie, W. Wu, J. Wu, *et al.*, Comparison of Two Positions of Knee Arthrocentesis, *Am. J. Phys. Med. Rehabil.*, 2012, **91**, 611–615.
12 A. J. Seidman and F. Limaiem, *Synovial Fluid Analysis*, 2019, https://www.ncbi.nlm.nih.gov/books/NBK537114/.
13 C. Deirmengian, S. Feeley, G. S. Kazarian and K. Kardos, Synovial Fluid Aspirates Diluted with Saline or Blood Reduce the Sensitivity of Traditional and Contemporary Synovial Fluid Biomarkers, *Clin. Orthop. Relat. Res.*, 2020, **478**, 1805–1813.
14 S. Roberts, H. Evans, K. Wright, L. van Niekerk, B. Caterson, J. B. Richardson, *et al.*, ADAMTS-4 activity in synovial fluid as a biomarker of inflammation and effusion, *Osteoarthritis Cartilage*, 2015, **23**, 1622–1626.
15 F. Oliviero and B. F. Mandell, Synovial Fluid analysis: Relevance for Daily Clinical Practice, *Best Pract. Res., Clin. Rheumatol.*, 2023, **37**, 101848.
16 X. Wang, D. J. Hunter, X. Jin and C. Ding, The importance of synovial inflammation in osteoarthritis: current evidence from imaging assessments and clinical trials, *Osteoarthritis Cartilage*, 2018, **26**, 165–174.
17 P. Yin, A. Peter, H. Franken, X. Zhao, S. S. Neukamm, L. Rosenbaum, *et al.*, Preanalytical aspects and sample quality assessment in metabolomics studies of human blood, *Clin. Chem.*, 2013, **59**, 833–845.
18 M. Beattie and O. A. H. Jones, Rate of Advancement of Detection Limits in Mass Spectrometry: Is there a Moore's Law of Mass Spec?, *ass Spectrom.*, 2023, **12**, A0118.
19 V. B. Kraus, T. V. Stabler, S. Y. Kong, G. Varju and G. McDaniel, Measurement of synovial fluid volume using urea, *Osteoarthritis Cartilage*, 2007, **15**, 1217–1220.
20 D. Mazzucco, R. Scott and M. Spector, Composition of joint fluid in patients undergoing total knee replacement and revision arthroplasty: correlation with flow properties, *Biomaterials*, 2004, **25**, 4433–4445.
21 A. S. Mann, A. M. Smith, J. O. Saltzherr, A. Gopinath and R. C. Andresen Eguiluz, Glycosaminoglycans and glycoproteins influence the elastic response of synovial fluid nanofilms on model oxide surfaces, *Colloids Surf., B*, 2022, **213**, 112407.
22 S. Y. Song, Y. D. Han, S. Y. Hong, K. Kim, S. S. Yang, B.-H. Min, *et al.*, Chip-based cartilage oligomeric matrix protein detection in serum and synovial fluid for osteoarthritis diagnosis, *Anal. Biochem.*, 2011, **420**, 139–146.
23 P. Tsirtoglou, E. Thursby, C. Phillips and D. Harvey, 36 Investigating the utility of hyaluronidase treatment in prosthetic joint fluid analysis, to improve the diagnostic workflow, *Clin. Infect. Pract.*, 2023, **20**, 100297.
24 H. Brouwers, J. H. von Hegedus, E. van der Linden, R. Mahdad, M. Kloppenburg, R. Toes, *et al.*, Hyaluronidase treatment of synovial fluid is required for accurate detection of inflammatory cells and soluble mediators, *Arthritis Res. Ther.*, 2022, **24**(1), DOI: 10.1186/s13075-021-02696-4.
25 H. M. Gegner, T. Naake, A. Dugourd, T. Müller, F. Czernilofsky, G. Kliewer, *et al.*, Pre-analytical processing of plasma and serum samples for combined proteome and metabolome analysis, *Front. Mol. Biosci.*, 2022, **9**, DOI: 10.3389/fmolb.2022.961448.
26 P. Bernini, I. Bertini, C. Luchinat, P. Nincheri, S. Staderini and P. Turano, Standard operating procedures for pre-analytical handling of blood and urine for metabolomic studies and biobanks, *J. Biomol. NMR*, 2011, **49**, 231–243.
27 M. V. Fomenko, L. V. Yanshole and Y. P. Tsentalovich, Stability of Metabolomic Content during Sample Preparation: Blood and Brain Tissues, *Metabolites*, 2022, **12**, 811.
28 O. Teahan, S. Gamble, E. Holmes, J. Waxman, J. K. Nicholson, C. Bevan, *et al.*, Impact of Analytical Bias in Metabonomic Studies of Human Blood Serum and Plasma, *Anal. Chem.*, 2006, **78**, 4307–4318.
29 Y. Zhang, S. Zhang, Y. Zhang, Q. Nie and L. Shen, Exploring morphological effects and multi–scale analysis on the mechanical properties and volume stability of composite mortar, *Case Stud. Constr. Mater.*, 2013, **21**, e03808.
30 A. Z. Damyanovich, J. R. Staples and K. W. Marshall, The effects of freeze/thawing on human synovial fluid observed by 500 MHz 1H magnetic resonance spectroscopy, *PubMed*, 2000, **27**, 746–752.
31 J. R. Anderson, M. M. Phelan, L. M. Rubio-Martinez, M. M. Fitzgerald, S. W. Jones, P. D. Clegg, *et al.*, Optimization of Synovial Fluid Collection and Processing for NMR Metabolomics and LC-MS/MS Proteomics, *J. Proteome Res.*, 2020, **19**, 2585–2597.
32 M. K. J. Jaggard, C. L. Boulangé, G. Graça, P. Akhbari, U. Vaghela, R. Bhattacharya, *et al.*, The influence of sample collection, handling and low temperature storage upon NMR metabolic profiling analysis in human synovial fluid, *J. Pharm. Biomed. Anal.*, 2021, **197**, 113942.
33 J. Figueira, S. Gouveia-Figueira, C. Öhman, P. Lif Holgerson, M. L. Nording and A. Öhman, Metabolite quantification by NMR and LC-MS/MS reveals differences between unstimulated, stimulated, and pure parotid saliva, *J. Pharm. Biomed. Anal.*, 2017, **140**, 295–300.
34 G. A. N. Gowda, W. Zhu and D. Raftery, NMR-based metabolomics: Where are we now and where are we going?, *Prog. Nucl. Magn. Reson. Spectrosc.*, 2025, 101564.
35 D. Malmodin, A. Bay Nord, H. Zafar, L. Paulson, B. G. Karlsson and Å. T. Naluai, Preanalytical (Mis) Handling of Plasma Investigated by 1 H NMR Metabolomics, *ACS Omega*, 2024, **9**, 48727–48737.
36 M. Khadka, A. Todor, K. M. Maner-Smith, J. K. Colucci, V. Tran, D. A. Gaul, *et al.*, The Effect of Anticoagulants, Temperature, and Time on the Human Plasma Metabolome and Lipidome from Healthy Donors as

Open Access Article. Published on 21 January 2026. Downloaded on 2/26/2026 9:07:48 AM. This article is licensed under a Creative Commons Attribution-NonCommercial 3.0 Unported Licence.

Determined by Liquid Chromatography-Mass Spectrometry, *Biomolecules*, 2019, **9**, 200.

37 M. R. La, S. L. Carmichael, C. Ma, M. Hardley, T. Shen, R. Wong, *et al.*, Impact of post-collection freezing delay on the reliability of serum metabolomics in samples reflecting the California mid-term pregnancy biobank, *Metabolomics*, 2018, **14**(11), DOI: 10.1007/s11306-018-1450-9.

38 V. Ghini, P. M. Abuja, O. Polasek, L. Kozera, P. Laiho, G. Anton, *et al.*, Impact of the pre-examination phase on multicenter metabolomic studies, *New Biotechnol.*, 2022, **68**, 37–47.

39 Ö. C. Zeki, C. C. Eylem, T. Reçber, S. Kır and E. Nemutlu, Integration of GC-MS and LC-MS for untargeted metabolomics profiling, *J. Pharm. Biomed. Anal.*, 2020, **190**, 113509.

40 V. L. Stevens, E. Hoover, Y. Wang and K. A. Zanetti, Pre-Analytical Factors that Affect Metabolite Stability in Human Urine, Plasma, and Serum: A Review, *Metabolites*, 2019, **9**, 156.

41 W. B. Dunn, D. Broadhurst, P. Begley, E. Zelena, S. Francis-McIntyre, N. Anderson, *et al.*, Procedures for large-scale metabolic profiling of serum and plasma using gas chromatography and liquid chromatography coupled to mass spectrometry, *Nat. Protoc.*, 2011, **6**, 1060–1083.

42 L. W. Sumner, A. Amberg, D. Barrett, M. H. Beale, R. Beger, C. A. Daykin, *et al.*, Proposed minimum reporting standards for chemical analysis, *Metabolomics*, 2007, **3**, 211–221.

43 P. Yin, R. Lehmann and G. Xu, Effects of pre-analytical processes on blood samples used in metabolomics studies, *Anal. Bioanal. Chem.*, 2015, **407**, 4879–4892.

44 I. Popović, L. Dončević, R. Biba, K. Košpić, M. Barbalić, M. Marinković, *et al.*, Advancements in Adenine Nucleotides Extraction and Quantification from a Single Drop of Human Blood, *Molecules*, 2024, **29**, 5630.

45 N. Gowda, V. Pascua, L. Hill, D. Djukovic, D. Wang and D. Raftery, Discovery of Hypoxanthine and Inosine as Robust Biomarkers for Predicting the Preanalytical Quality of Human Plasma and Serum for Metabolomics, *Anal. Chem.*, 2024, **96**(39), DOI: 10.1021/acs.analchem.4c03719.

46 M. Furuhashi, New insights into purine metabolism in metabolic diseases: role of xanthine oxidoreductase activity, *Am. J. Physiol.: Endocrinol. Metab.*, 2020, **319**, E827–E834.

47 H. Sekizuka, Uric acid, xanthine oxidase, and vascular damage: potential of xanthine oxidoreductase inhibitors to prevent cardiovascular diseases, *Hypertens. Res.*, 2022, **45**(5), 772–774.

48 G. Guazzelli, R. Lazzaroni and R. Settambolo, Synthesis of (–)-Indolizidine 167B based on domino hydroformylation/cyclization reactions, *Beilstein J. Org. Chem.*, 2008, **4**, DOI: 10.1186/1860-5397-4-2.

49 C. K. Phwan, H. C. Ong, W.-H. Chen, T. C. Ling, E. P. Ng and P. L. Show, Overview: Comparison of pretreatment technologies and fermentation processes of bioethanol from microalgae, *Energy Convers. Manage.*, 2018, **173**, 81–94.

50 P. E. Kelly, H. J. Ng, G. Farrell, S. McKirdy, R. K. Russell, R. Hansen, *et al.*, An Optimised Monophasic Faecal Extraction Method for LC-MS Analysis and Its Application in Gastrointestinal Disease, *Metabolites*, 2022, **12**, 1110.

51 M. Höring, S. Krautbauer, L. Hiltl, V. Babl, A. Sigruener, R. Burkhardt, *et al.*, Accurate Lipid Quantification of Tissue Homogenates Requires Suitable Sample Concentration, Solvent Composition, and Homogenization Procedure—A Case Study in Murine Liver, *Metabolites*, 2021, **11**, 365.

52 E. A. Zelentsova, V. V. Yanshole and Y. P. Tsentalovich, A novel method of sample homogenization with the use of a microtome-cryostat apparatus, *RSC Adv.*, 2019, **9**, 37809–37817.

53 Z. E. Wu, M. C. Kruger, G. J. S. Cooper, S. D. Poppitt and K. Fraser, Tissue-Specific Sample Dilution: An Important Parameter to Optimise Prior to Untargeted LC-MS Metabolomics, *Metabolites*, 2019, **9**, 124.

54 F. Dieterle, A. Ross, G. Schlotterbeck and H. Senn, Probabilistic Quotient Normalization as Robust Method to Account for Dilution of Complex Biological Mixtures. Application in ^{1}H NMR Metabonomics, *Anal. Chem.*, 2006, **78**, 4281–4290.

55 C. Jayadev, S. Snelling, D. Mahoney, A. Price and P. Hulley, Hyaluronidase treatment of synovial fluid can improve measured signal by multiplex immunoassay platforms, *Osteoarthritis Cartilage*, 2013, **21**, S81.

This journal is © The Royal Society of Chemistry 2026